

pubs.acs.org/est Article

# Which Surface Is More Scaling Resistant? A Closer Look at Nucleation Theories for Heterogeneous Gypsum Nucleation in Aqueous Solutions

Yiming Yin, Tianshu Li, Kuichang Zuo, Xitong Liu, Shihong Lin, Yiqun Yao, and Tiezheng Tong\*



Cite This: Environ. Sci. Technol. 2022, 56, 16315-16324



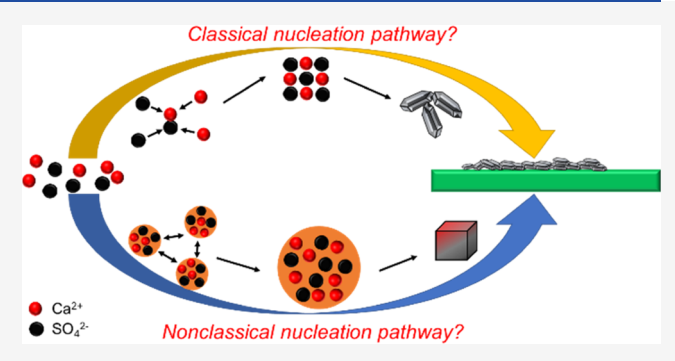
**ACCESS** I

Metrics & More

Article Recommendations

Supporting Information

ABSTRACT: Developing engineered surfaces with scaling resistance is an effective means to inhibit surface-mediated mineral scaling in various industries including desalination. However, contrasting results have been reported on the relationship between scaling potential and surface hydrophilicity. In this study, we combine a theoretical analysis with experimental investigation to clarify the effect of surface wetting property on heterogeneous gypsum (CaSO $_4$ ·2 $H_2$ O) formation on surfaces immersed in aqueous solutions. Theoretical prediction derived from classical nucleation theory (CNT) indicates that an increase of surface hydrophobicity reduces scaling potential, which contrasts our experimental results that more hydrophilic surfaces are less prone



to gypsum scaling. We further consider the possibility of nonclassical pathway of gypsum nucleation, which proceeds by the aggregation of precursor clusters of CaSO<sub>4</sub>. Accordingly, we investigate the affinity of CaSO<sub>4</sub> to substrate surfaces of varied wetting properties *via* calculating the total free energy of interaction, with the results perfectly predicting experimental observations of surface scaling propensity. This indicates that the interactions between precursor clusters of CaSO<sub>4</sub> and substrate surfaces might play an important role in regulating heterogeneous gypsum formation. Our findings provide evidence that CNT might not be applicable to describing gypsum scaling in aqueous solutions. The fundamental insights we reveal on gypsum scaling mechanisms have the potential to guide rational design of scaling-resistant engineered surfaces.

KEYWORDS: mineral scaling, surface wetting property, classical nucleation theory, total free energy of interaction, nonclassical nucleation pathway

#### **■** INTRODUCTION

Mineral nucleation is a widely observed phenomenon in environmental science, mineralogy, and materials science. <sup>1–6</sup> Mineral nucleation can take place *via* homogeneous nucleation in the bulk solution or heterogeneous nucleation if foreign substrates are present. Particularly, heterogeneous nucleation has attracted great attention due to its strong relevance to and significant impact on numerous applications. <sup>2,7–10</sup> In desalination, for example, *in situ* surface formation of mineral nuclei on the membrane surface not only shortens the lifespan of the membrane materials but also compromises desalination efficiency. <sup>11,12</sup> Therefore, elucidating the mechanisms of mineral nucleation, particularly its fundamental relationship with surface properties, is of essential importance to developing effective strategies for scaling mitigation and fabricating engineered surfaces that are capable of reducing, and ideally eliminating, scale accumulation. <sup>7,8</sup>

The propensity of nucleation is typically described by classical nucleation theory (CNT), which is a widely used theoretical framework for explaining crystallization phenomena. CNT quantifies the change of Gibbs free energy

 $(\Delta G)$  for nucleus formation, <sup>6,18</sup> which is determined by the free-energy change arising from the formation of the bulk mineral and the energy penalty due to the increase of interfacial area. <sup>6,7</sup> The value of  $\Delta G$  reaches its maximum when the nucleus grows to a critical size, thereby creating a free-energy barrier to mineral nucleation.

The theoretical framework of CNT has been adopted by studies of membrane desalination for the development of scaling-resistant membranes.<sup>19–21</sup> However, contradictory results have been reported regarding how surface wetting property (*i.e.*, if the surface is hydrophilic or hydrophobic) regulates the membrane propensity to mineral scaling. Certain studies suggest that increasing surface hydrophobicity

Received: September 8, 2022 Revised: October 18, 2022 Accepted: October 19, 2022 Published: October 28, 2022





enhances the free-energy barrier for heterogeneous nucleation and thus delays scale formation on the membrane materials, <sup>19–22</sup> whereas others conversely demonstrate that increasing surface hydrophilicity, rather than hydrophobicity, is an effective strategy to deter scale formation on solid surfaces. <sup>23–27</sup> This inconsistency creates a controversy on the relationship between scaling potential and surface wetting property, prompting further elucidation of the factors that regulate heterogeneous nucleation of mineral scales.

Furthermore, CNT was initially developed to investigate the condensation of water vapor. 28-30 While it has been further applied to other systems such as mineral crystallization in aqueous solutions and ice nucleation on surfaces, 17,31,32 crystallization in nature does not always follow CNT. 17,33,34 Nonclassical nucleation pathways involving the aggregation of prenucleation or precursor clusters have been proposed.<sup>35–37</sup> These stable clusters are considered at local free-energy minimum, thereby contradicting the assumption of CNT that the nucleus is stable only if its size exceeds the critical size. 17,34 Therefore, a closer look at the applicability of CNT to describing surface-induced mineral scaling is needed. Also, it is worth to mention that the term prenucleation cluster (PNC) is typically used for the formation of calcite in the literature. 35,38 For other minerals such as gypsum, it is not conclusive whether the CaSO<sub>4</sub> clusters should be defined as PNC.<sup>37</sup> As a result, the term precursor cluster, which is more accurate for describing the nascent intermediates in the nonclassical pathway of gypsum formation,<sup>37,39</sup> will be used along this manuscript.

In this work, we investigate the relationship between scaling potential and surface wetting property in aqueous solutions using a combination of theoretical and experimental approaches. Gypsum scaling was selected as the representative scaling type due to its common presence in desalination systems. 6,40 We first revisit the theory of CNT to derive the relationship between the free-energy barrier of surfacemediated gypsum nucleation and surface wetting property. The validity of this relationship was investigated by experimental results of surface scaling propensity. Inspired by the concept of precursor clusters in the nonclassical nucleation pathway, we further explored the affinity of CaSO<sub>4</sub> with substrate surfaces of varied wetting properties via calculating the total free energy of interaction, which was correlated to the extent of gypsum scaling. Our study provides evidence that CNT might not be applicable to describing gypsum scale formation in aqueous solutions. Instead, heterogeneous nucleation of gypsum might be regulated by the interactions of precursor clusters with the substrate surface. The implications of our findings to the design of scaling-resistant surfaces (e.g., for membrane desalination) are also discussed.

#### MATERIALS AND METHODS

The glass substrates were purchased from Capitol Scientific (Austin, TX). Pure ethanol (200 proof) was provided by Decon Laboratories (King of Prussia, PA). Calcium chloride dihydrate ( $CaCl_2 \cdot 2H_2O$ ), sodium sulfate ( $Na_2SO_4$ ), and n-hexane were acquired from Fisher Chemical (Hampton, NH). Ethylene glycol and diiodomethane were purchased from Sigma Aldrich (St. Louis, MO). Hexyltriethoxysilane ( $C_{12}H_{28}O_3Si$ , 97%), n-decyltriethoxysilane ( $C_{16}H_{36}O_3Si$ , 97%), and (heptadecafluoro-1,1,2,2-tetrahydrodecyl)-triethoxysilane ( $C_{16}H_{19}F_{17}O_3Si$ , 97%) were obtained from

Gelest (Morrisville, PA). Deionized (DI) water was supplied from a water purification system (>18 M $\Omega$ , Millipore).

Preparation of Glass Substrates with Different Surface Functionalities. Glass substrates with different functional groups were obtained via grafting three functional silanes on the surface of glass substrates, respectively. Before surface modification, all glass substrates were thoroughly rinsed by DI water and pure ethanol, followed by a 15-min sonication treatment. The functional silanes, each terminated with ethoxy groups, can hydrolyze to form a silanol group and react with the hydroxy groups on the glass substrate surface. 41 In brief, the glass substrates were immersed in 1 v/v % silane/n-hexane solution for 24 h with gentle mixing. After the reaction, the resultant silane-grafted glass substrates were thoroughly rinsed with n-hexane to remove the unreacted silane molecules and air-dried under room temperature. The surfaces of the glass substrates grafted with hexyltriethoxysilane, n-decyltriethoxysilane, and (heptadecafluoro-1,1,2,2-tetrahydrodecyl)triethoxysilane were denoted as CH<sub>3</sub>/C<sub>6</sub>, CH<sub>3</sub>/C<sub>10</sub>, and  $CF_3/C_{10}$ , respectively, where  $C_6$  and  $C_{10}$  represent the number of carbon atoms of the molecule backbone (i.e., the length of the silane molecule anchored on the substrate surface).

**Substrate Surface Characterization.** The surface hydrophilicity and the surface energy of the glass substrates (both unmodified and modified) were characterized by measuring the contact angles (CAs) of specific probe liquids using the sessile method with a goniometer (Ramé-hart Instrument Corporation, Succasunna, NJ). Specifically, water, ethylene glycol, and diiodomethane were used as the probe liquids with known surface tension components (Table S1, Supporting Information). An 8  $\mu$ L liquid droplet was placed on the surface of the substrate, with the measurement performed after the liquid droplet was stabilized for 10 s. The CA measurement was carried out at three different locations of each substrate, and the average values of CA  $\pm$  the standard deviations are reported (Figure S1, Supporting Information). With the  $CA(\theta)$  between the three probe liquids and the substrate surface, we calculated the surface energy components stemming from the Lifshitz-van der Waals  $(\gamma_S^{LW})$  and Lewis acid-base  $(\gamma_S^+, \gamma_S^-)$  interactions for each glass substrate using 42

$$(1 + \cos \theta)\gamma_{\rm L} = 2(\sqrt{\gamma_{\rm S}^{\rm LW}\gamma_{\rm L}^{\rm LW}} + \sqrt{\gamma_{\rm S}^{+}\gamma_{\rm L}^{-}} + \sqrt{\gamma_{\rm S}^{-}\gamma_{\rm L}^{+}}) \tag{1}$$

where  $\gamma_{\rm L}^{\rm LW}$ ,  $\gamma_{\rm L}^+$ , and  $\gamma_{\rm L}^-$  represent the Lifshitz–van der Waals surface tension component, electron–acceptor, and electron–donor surface tension components of the probe liquids, respectively;  $\gamma_{\rm L}$  denotes the total surface tension of the probe liquids; and  $\gamma_{\rm S}^{\rm LW}$ ,  $\gamma_{\rm S}^+$ , and  $\gamma_{\rm S}^-$  represent surface energy components of substrate surfaces (Table S2, Supporting Information). In addition, the surface chemical compositions of the unmodified substrate and the substrates grafted with different functional silanes were analyzed by X-ray photoelectron spectroscopy (XPS) using a PHI-5800 spectrometer (Physics Electronics, Chanhassen, MN) with a monochromatic Al-K X-ray source. The spectra of the substrate samples were calibrated based on the adventitious carbon C 1s, which is assigned to the value of 284.8 eV.

Scaling Experiments of Heterogeneous Gypsum Nucleation. Static scaling experiments were performed to assess the propensity of each glass substrate to gypsum scaling. Gypsum solutions were prepared by mixing 25 mM  $CaCl_2$ ·  $2H_2O$  and 25 mM  $Na_2SO_4$  in DI water at room temperature  $(20 \pm 0.5 \, ^{\circ}C)$ , resulting in a saturation index (SI, defined as

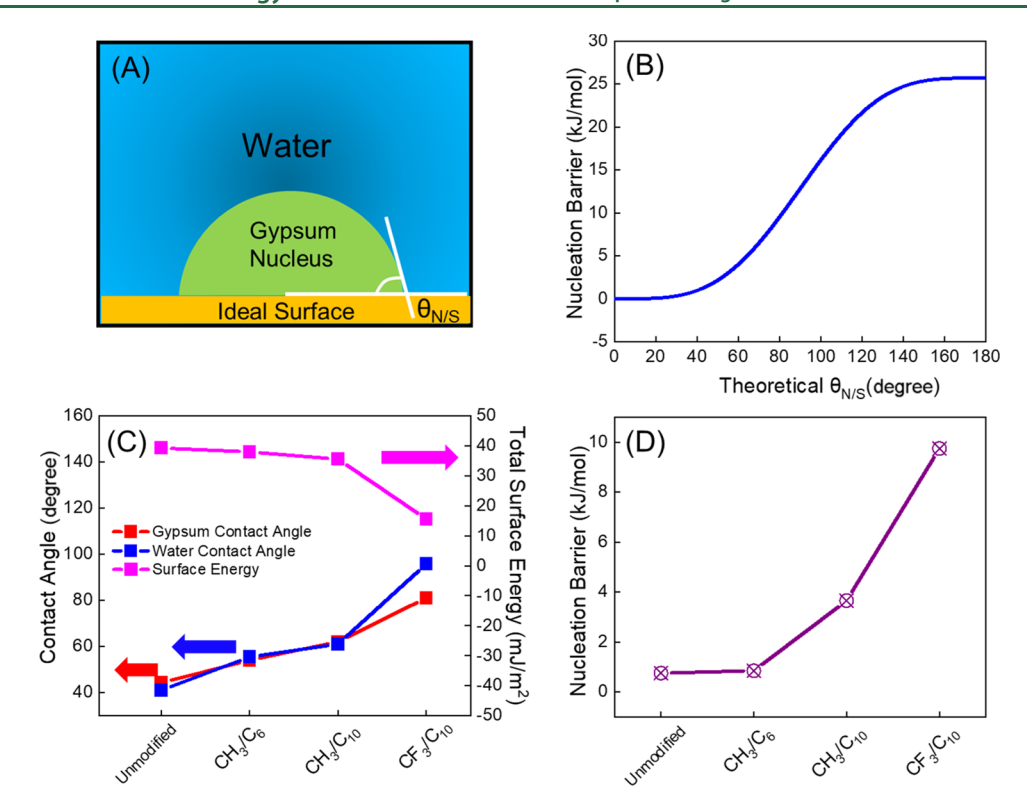


Figure 1. Propensities of different substrates to gypsum scaling as predicted by CNT. (A) Geometrical illustration of a hemisphere gypsum nucleus on an ideal solid surface. (B) Positive correlation between the theoretical contact angle  $\theta_{\rm N/S}$  and the free-energy barrier of gypsum nucleation. (C) Contact angles  $\theta_{\rm N/S}$  (calculated, red line), total surface energy (calculated, pink line), and water contact angles (measured, blue line) of the substrates. (D) Calculated free-energy barriers of gypsum heterogeneous nucleation for the unmodified substrate (with the –OH group) and the CH<sub>3</sub>/C<sub>6</sub>-, CH<sub>3</sub>/C<sub>10</sub>-, and CF<sub>3</sub>/C<sub>10</sub>-modified substrate surfaces, respectively (–OH is from the unmodified glass slides, CH<sub>3</sub>/C<sub>6</sub> is from hexyltriethoxysilane, CH<sub>3</sub>/C<sub>10</sub> is from *n*-decyltriethoxysilane, and CF<sub>3</sub>/C<sub>10</sub> is from (heptadecafluoro-1,1,2,2-tetrahydrodecyl)triethoxysilane).

the natural logarithm of the ratio between ion activity product and solubility equilibrium constant,  $ln(IAP/K_{sp})$ ) of gypsum at 0.44, as calculated by PHREEQC software and the WATEQ4F database (PC version).44 Both the unmodified and modified glass substrates were immersed vertically in the gypsum solution (800 mL) at room temperature (20  $\pm$  0.5 °C). A magnetic stirring bar was used to mix the solution at 450 rpm. The gypsum scaling experiment lasted for 2 days, after which all samples were gently washed by the experiment solution and dried in the oven (50 °C). The gypsum scale coverage of each glass substrate was quantified using ImageJ software (National Institutes of Health) to determine the extent of scale formation. The original optical images were first converted to binary (i.e., white and black) images. Then, the fractions of gypsum scale coverage on different surfaces after scaling experiments were calculated automatically by ImageJ using brightness values.45

#### ■ RESULTS AND DISCUSSION

Increase of Surface Hydrophobicity Enhances Scaling Resistance According to Classical Nucleation Theory. In CNT, the height of free-energy barrier to heterogeneous nucleation is determined by the interplay between the bulk free energy and the interfacial free energy 6,7,46

$$\Delta G = -n\Delta\mu + A\gamma \tag{2}$$

where n is the number of crystal repeating units in the nucleus;  $\gamma$  and A refer to the interfacial energy and contact area between the nucleus and the surrounding medium, respectively; and  $\Delta\mu$  is the change in chemical potential when a crystal repeating

unit enters the crystal phase from the solution phase, which can be calculated as follows

$$\Delta \mu = k_{\rm B} T \ln \left( \frac{\rm IAP}{K_{\rm sp}} \right) \tag{3}$$

where  $k_{\rm B}$  and T are Boltzmann constant (1.38  $\times$  10<sup>-20</sup> mJ/K) and the absolute temperature (K), respectively; IAP is the ion activity product; and  $K_{\rm sp}$  is the solubility product. Equation 2 can be further expanded according to the

Equation 2 can be further expanded according to the geometrical relations of a hemispherical nucleus with an ideal surface (Figure 1A), yielding the following equation (the detailed derivation is described in the Supporting Information, Text S1)

$$\Delta G_{\text{het}}^* = -\frac{\pi R^{*3} (1 - \cos \theta_{\text{N/S}})^2 (2 + \cos \theta_{\text{N/S}})}{3} \frac{\Delta \mu}{\Omega} + 2\pi R^{*2} (1 - \cos \theta_{\text{N/S}}) \gamma_{\text{N/W}} + \pi R^{*2} \sin^2 \theta_{\text{N/S}} (\gamma_{\text{N/S}} - \gamma_{\text{W/S}})$$
(4)

where  $R^*$  is the critical radius of the nucleus, which can be derived when the derivative of Gibbs nucleation free energy with respect to the nucleus radius equals to zero;  $\theta_{\mathrm{N/S}}$  is the contact angle between the nucleus and the surface, which is different from  $\theta$  used in eq 1 (i.e., the contact angle between the probe liquid and the substrate surface);  $\gamma_{\mathrm{N/W}}$  and  $\gamma_{\mathrm{N/S}}$  are the interfacial tensions of the mineral nucleus with water and the substrate surface, respectively; and  $\gamma_{\mathrm{W/S}}$  refers to the interfacial tension between water and the substrate surface.

To unify the terms associated with interfacial tensions in eq 4,  $\gamma_{\rm N/W}$ ,  $\gamma_{\rm N/S}$ , and  $\gamma_{\rm W/S}$  can be correlated using the Dupré–Young equation.<sup>6,7</sup>

$$\gamma_{W/S} - \gamma_{N/S} = \cos \theta_{N/S} \gamma_{N/W} \tag{5}$$

With eq 5, eq 4 can be rearranged as follows

$$\Delta G_{\text{het}}^* = -\frac{\pi R^{*3} (1 - \cos \theta_{\text{N/S}})^2 (2 + \cos \theta_{\text{N/S}})}{3} \frac{\Delta \mu}{\Omega} + \pi R^{*2} (2 - 2 \cos \theta_{\text{N/S}} - \sin^2 \theta_{\text{N/S}} \cos \theta_{\text{N/S}})$$

$$\gamma_{\text{N/W}}$$
(6

A close look at eq 6 reveals that (1) the bulk free energy (i.e., the first term on the right side of eq 6) remains negative under a supersaturated condition (i.e., it favors the formation of nuclei) and (2) the surface-area-dependent term (i.e., the second term on the right side of eq 6) is a function of the contact angle  $\theta_{\rm N/S}$  for a given interfacial tension between the nucleus and water,  $\gamma_{N/W}$  (Figure S2, Supporting Information). Here, we used gypsum (CaSO<sub>4</sub>·2H<sub>2</sub>O) as the model mineral and calculated its free-energy barriers for heterogeneous nucleation as a function of  $\theta_{\mathrm{N/S}}$ . Evaluating the free-energy barrier requires knowing  $\gamma_{N/W}$  which, for gypsum and water, has a range of 5.8-100 mJ/m<sup>2</sup> as reported.<sup>47</sup> In our calculation, we selected the value of 8.9 mJ/m<sup>2</sup>, which was derived from measuring the induction time of gypsum, 48 to compute the corresponding free-energy barriers of gypsum for different substrate surfaces because the calculated values of free-energy barriers are comparable with the literature. 49 As shown in Figure 1B, a positive correlation between the freeenergy barrier of heterogeneous nucleation and  $\theta_{
m N/S}$  was observed (it is worth mentioning that such a positive correlation is still valid for other values of  $\gamma_{N/W}$  within the range of 5.8-100 mJ/m<sup>2</sup>). Thus, according to CNT, a substrate surface results in a higher free-energy barrier to gypsum nucleation if the contact angle between the nucleus and the substrate surface,  $\theta_{N/S}$ , is higher.

Although  $\Delta G_{\rm het}^*$  can be evaluated using  $\theta_{\rm N/S}, \; \theta_{\rm N/S}$  is a hypothetical parameter and cannot be measured experimentally. To connect  $\theta_{\rm N/S}$  with measurable properties of material surface, we use eq 7 to correlate  $\theta_{\rm N/S}$  with the apolar and polar surface energy components (i.e.,  $\gamma^{\rm LW}, \; \gamma^+, \; \gamma^-)^{42}$ 

$$\cos \theta_{\text{N/S}} = \frac{2(\sqrt{\gamma_{\text{S}}^{\text{LW}} \gamma_{\text{N}}^{\text{LW}}} + \sqrt{\gamma_{\text{S}}^{+} \gamma_{\text{N}}^{-}} + \sqrt{\gamma_{\text{S}}^{-} \gamma_{\text{N}}^{+}})}{\gamma_{\text{N}}} - 1 \tag{7}$$

$$\gamma_{S} = \gamma_{S}^{LW} + 2\sqrt{\gamma_{S}^{+}\gamma_{S}^{-}} \tag{8}$$

where  $\gamma_{\rm N}$  and  $\gamma_{\rm S}$  are the total surface energies of the nucleus and the substrate;  $\gamma_{\rm S}^{\rm LW}$  and  $\gamma_{\rm N}^{\rm LW}$  are the contribution of dispersion forces to the surface energy of the substrate and the nucleus; and  $\gamma_{\rm S}^{\rm t}$ ,  $\gamma_{\rm S}^{\rm t}$ ,  $\gamma_{\rm N}^{\rm t}$ , and  $\gamma_{\rm N}^{\rm t}$  are the electron—acceptor (designated as  $\gamma^{\rm t}$ ) and the electron—donor (designated as  $\gamma^{\rm t}$ ) surface energy components of the substrate and the nucleus (Tables S1 and S2), respectively. Here, we used experimental data to illustrate the relationship between  $\theta_{\rm N/S}$  and surface properties of the substrates. We calculated the values of  $\theta_{\rm N/S}$  with respect to the surfaces with different wetting properties and surface energies.

As shown in Figure 1C,  $\theta_{\text{N/S}}$  (calculated by eq 7, red line) negatively correlates with the substrate surface energy  $\gamma_{\text{S}}$  (calculated by eq 8, pink line), whereas it exhibits a positive

correlation with the water contact angle (blue line) that indicates the wetting property of the surface (also see Figure S3, Supporting Information). The changes of the surface energy and the water contact angle of different substrates were due to the different surface functional groups, which were confirmed by XPS analyses (Figure S4, Supporting Information). Therefore, a more hydrophobic surface (i.e., higher water contact angle) with a lower surface energy has a higher contact angle  $\theta_{
m N/S}$  for gypsum, which corresponds to a more positive free-energy barrier for heterogeneous gypsum nucleation (Figure 1B). Accordingly, increasing surface hydrophobicity theoretically hinders gypsum scaling by increasing the freeenergy barrier of heterogeneous nucleation within the framework of CNT. Conversely, more hydrophilic surfaces are more prone to gypsum scaling. These results are in accordance with the conclusion stated by several studies that superhydrophobic membranes are scaling resistant. 19-22 We note that several existing studies incorrectly substitute  $heta_{ ext{N/S}}$ with water contact angle when applying eqs 5 and 6. 19-21 This approach, although inaccurate in theory, should still result in a correct, qualitative conclusion due to the positive correlation between  $\theta_{N/S}$  and water contact angle as shown in Figure 1C. Our theoretical analysis presented above corrects the misuse of water contact angle for  $heta_{ ext{N/S}}$  but still demonstrates similar relationship between the wetting property and the scaling propensity of substrate surface within the framework of CNT, i.e., the surface-mediated gypsum formation is more favorable for hydrophilic surfaces rather than for hydrophobic surfaces.

We further quantified such a relationship by computing the free-energy barriers for heterogeneous gypsum nucleation on different substrates tested in this study. As shown in Figure 1D, the height of free-energy barriers for gypsum nucleation on substrates with different functional groups follows the order as the unmodified (with –OH, as shown by XPS analysis, Figure S4) < CH $_3/C_6$  < CH $_3/C_{10}$  < CF $_3/C_{10}$ . Specifically, the free-energy barrier for gypsum on the glass substrate terminated with CF $_3/C_{10}$  (~9.7 kJ/mol) is higher than other substrates (~0.8 to ~3.7 kJ/mol), which suggests the lowest propensity of the CF $_3/C_{10}$ -functionalized surface to gypsum scaling based on the CNT framework. The hydrophilic, unmodified substrate with –OH groups, which possesses the lowest free-energy barrier (~0.8 kJ/mol), is the most susceptible to gypsum scaling according to CNT.

Classical Nucleation Theory Does Not Predict Experimentally Measured Gypsum Scaling Propensity. To test the validity of CNT in predicting the relationship between surface scaling propensity and wetting property, we performed a series of static gypsum scaling experiments to investigate the scaling propensity of each substrate. In these experiments, both the unmodified and modified glass substrates were immersed vertically into a saturated gypsum solution with a SI of 0.44 for gypsum. With such a SI, homogeneous nucleation occurs after a long induction time (e.g., 7 days).<sup>23</sup> Considering that our experiments only lasted for 2 days, the contribution of homogeneous nucleation to gypsum scaling was negligible. To further verify this assumption, we measured the conductivity of the gypsumsupersaturated solution in the absence of glass substrates. The solution conductivity did not decrease with time within 2 days (Figure S5, Supporting Information), confirming that homogeneous nucleation of gypsum in the bulk solution did not occur.

After the scaling experiments, the extents of gypsum scaling on the substrate surfaces were quantified by evaluating the

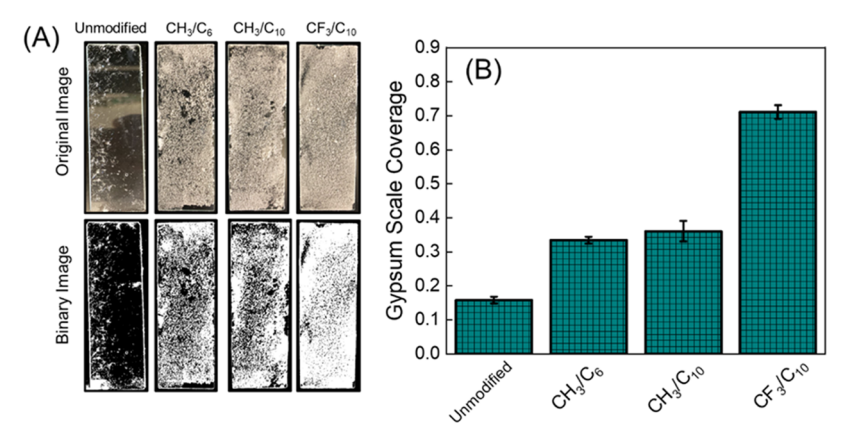


Figure 2. Results of static gypsum scaling experiments. (A) Optical images of the unmodified substrate (with the -OH group) and the  $CH_3/C_6$ ,  $CH_3/C_{10}$ , and  $CF_3/C_{10}$  substrate surfaces after 2 days of gypsum scaling experiments and their corresponding binary grayscale images analyzed by ImageJ. (B) Gypsum scale coverage for the unmodified substrate (with the -OH group) and the  $CH_3/C_6$ ,  $CH_3/C_{10}$ , and  $CF_3/C_{10}$ -modified substrate surfaces, respectively. The gypsum solution for the scaling experiments consisted of 25 mM  $CaCl_2$ - $2H_2O$  and 25 mM  $Na_2SO_4$ , corresponding to a SI value of 0.44 for gypsum. The error bars in (B) were obtained from three independent experiments.

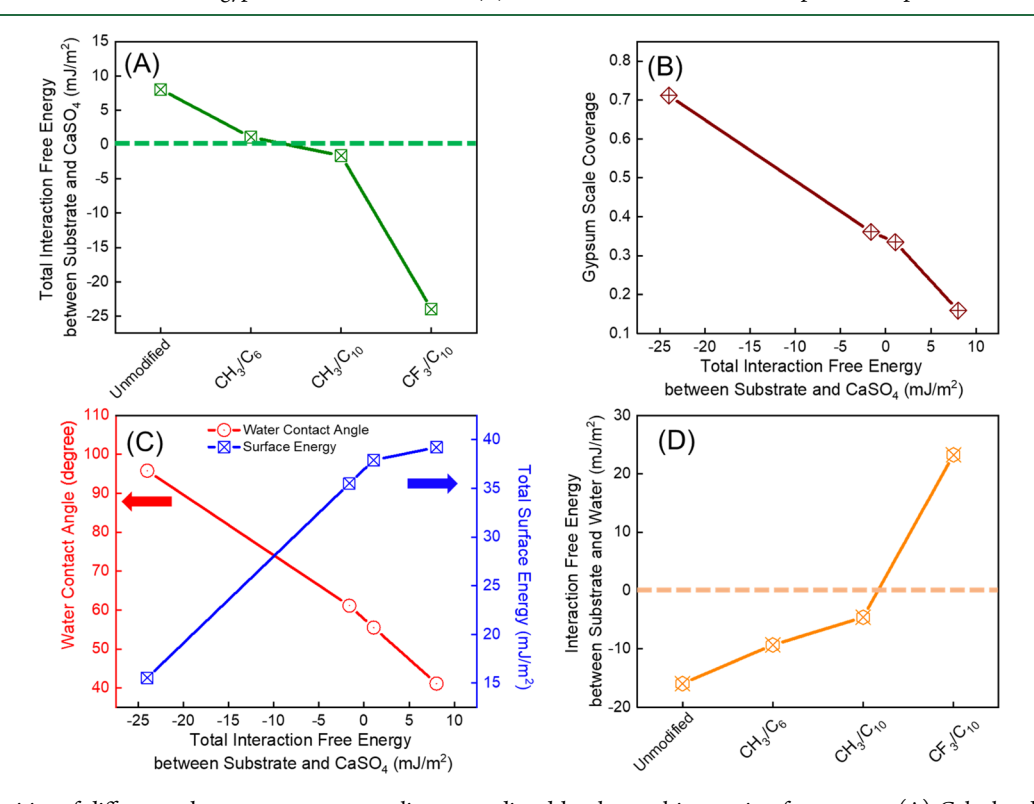


Figure 3. Propensities of different substrates to gypsum scaling as predicted by the total interaction free energy. (A) Calculated total interaction free energies between  $CaSO_4$  and the substrate surfaces terminated with -OH (unmodified),  $CH_3/C_6$ ,  $CH_3/C_{10}$ , and  $CF_3/C_{10}$  functional groups in water, respectively. (B) Negative correlation of the total interaction free energy (*i.e.*, between substrates and  $CaSO_4$ ) with gypsum scale coverage of the substrate surfaces. (C) Relationships of total interaction free energies (*i.e.*, between substrates and  $CaSO_4$ ) with water contact angle and total surface energy of the substrate surface. (D) Calculated interaction free energies of water with the substrate surfaces terminated with -OH,  $CH_3/C_6$ ,  $CH_3/C_{10}$ , and  $CF_3/C_{10}$  functional groups in aqueous solutions, respectively. The dashed lines in (A) and (D) represent the interaction free energy at value of 0 mJ/m<sup>2</sup>.

coverage of gypsum scales using ImageJ (Figure 2A). As shown in Figure 2B, all of the modified substrates showed a higher degree of scale coverage ( $\sim$ 33 to  $\sim$ 72%) than the unmodified glass substrate ( $\sim$ 16%). Among the three modified substrates, the CF<sub>3</sub>/C<sub>10</sub> substrate displayed the highest scale coverage ( $\sim$ 72%) after the scaling experiment, which was more than 30% higher than those of the CH<sub>3</sub>/C<sub>6</sub> ( $\sim$ 33%) and CH<sub>3</sub>/C<sub>10</sub> ( $\sim$ 36%) substrates. Therefore, the gypsum scale coverage on the substrates with different functional groups followed this

order: unmodified  $(-OH) < CH_3/C_6 < CH_3/C_{10} < CF_3/C_{10}$ , which was opposite to that of the scaling propensity predicted by CNT (Figure 1D). Thus, the combination of theoretical and experimental investigations in our study indicates that CNT might not be applicable to predicting surface propensity to gypsum scaling in aqueous solutions.

Free Energy of CaSO<sub>4</sub>-Surface Interaction under Water Can Predict Measured Gypsum Scaling Propensity. The gypsum scaling experiments in this study reveal the

limitation of CNT in predicting the scale formation propensity of surfaces with different wetting properties. The inconsistency between the theoretical prediction using CNT and the experimental results may be rooted in its assumptions. CNT assumes that the growth of the minerals is governed by the addition of one monomer (e.g., Ca2+ or SO42- ions for gypsum) at a time, with the collisions between multiple clusters into a larger aggregate being ignored within this theoretical framework.<sup>33</sup> However, this assumption stands in contrast to some experimental observations of gypsum crystallization reported. 30,51 Instead of being regulated by the classical ion-addition model, the nonclassical pathway of gypsum nucleation is a multistage process, which occurs via the aggregation of precursor clusters. 37,38,50,51 Such a nucleation transformation route, which suggests that the formation of gypsum crystals might proceed via an aggregation-based process, is considered as a nonclassical pathway of nucleation that is explained by the Ostwald rule of crystallization. 38,52 Therefore, the interactions between the CaSO<sub>4</sub> precursor clusters and the substrate surface may play an important role in controlling gypsum scale formation.

To investigate the affinity of CaSO<sub>4</sub> precursor clusters with surfaces of varied wetting properties, we calculated the free energy of interaction ( $\Delta G_{\text{C-W-S}}$ ) between CaSO<sub>4</sub> and the substrate surface in the medium of water as follows<sup>23,53</sup>

$$\begin{split} \Delta G_{\text{C-W-S}} &= 2[(\sqrt{\gamma_{\text{C}}^{\text{LW}}}\gamma_{\text{W}}^{\text{LW}} + \sqrt{\gamma_{\text{S}}^{\text{LW}}}\gamma_{\text{W}}^{\text{LW}} - \sqrt{\gamma_{\text{C}}^{\text{LW}}}\gamma_{\text{S}}^{\text{LW}} \\ &- \gamma_{\text{W}}^{\text{LW}}) + \sqrt{\gamma_{\text{W}}^{+}}(\sqrt{\gamma_{\text{C}}^{-}} + \sqrt{\gamma_{\text{S}}^{-}} - \sqrt{\gamma_{\text{W}}^{-}}) \\ &+ \sqrt{\gamma_{\text{W}}^{-}}(\sqrt{\gamma_{\text{C}}^{+}} + \sqrt{\gamma_{\text{S}}^{+}} - \sqrt{\gamma_{\text{W}}^{+}}) - \sqrt{\gamma_{\text{C}}^{+}}\gamma_{\text{S}}^{-} \\ &- \sqrt{\gamma_{\text{C}}^{-}}\gamma_{\text{S}}^{+}] \end{split}$$
(9)

where the subscripts C, W, and S stand for cluster, water, and substrate, respectively;  $\Delta G_{C-W-S}$  denotes the total interaction free energy between the cluster and the substrate surface in water;  $\gamma^{L \widecheck{W}}, \ \gamma^+, \ \text{and} \ \gamma^-$  are the Lifshitz-van der Waals surface energy component, electron-acceptor, and electron-donor surface energy components for each material. Although it has been reported that amorphous CaSO<sub>4</sub> and bassanite (CaSO<sub>4</sub>·  $0.5H_2O$ ) might form as intermediates during gypsum formation,  $^{50,51}$  there is a lack of reliable data for surface energy components of amorphous CaSO<sub>4</sub> and bassanite in the literature. Thus, the surface energy components of gypsum, which were accurately measured at the cleaved selenite plane (selenite is one variety of gypsum, whose (101) plane is the particular crystallographic plane that can be accurately cleaved),<sup>54</sup> were used in our calculation (Table S1). To the best of our knowledge, these values represent the most reliable data associated with surface energy components of CaSO<sub>4</sub>.

Using the surface energy components of substrate surfaces with different wetting properties (Table S2), we calculated  $\Delta G_{\text{C-W-S}}$  for various surfaces with different functional groups. As shown in Figure 3A, the total free energies of interaction between CaSO<sub>4</sub> and substrate surface are approximately 8.0, 1.1, -1.7, and -24.0 mJ/m² for the unmodified glass substrate (with the -OH functional group) and the CH<sub>3</sub>/C<sub>6</sub>-, CH<sub>3</sub>/C<sub>10</sub>-, and CF<sub>3</sub>/C<sub>10</sub>-modified substrate surfaces, respectively. Specifically, the free energy of interaction of CaSO<sub>4</sub> with the unmodified glass substrate (8.0 mJ/m²) was more positive than those with other substrates (from 1.1 to -24.0 mJ/m²), which suggests that the adhesion of CaSO<sub>4</sub> onto the unmodified glass substrate is the least favorable. Among the three modified

substrate surfaces, the CF<sub>3</sub>/C<sub>10</sub>-modified surface showed the most negative interaction free energy  $(-24.0 \text{ mJ/m}^2)$ , indicating its highest affinity with CaSO<sub>4</sub>. Assuming that adhesion of CaSO<sub>4</sub> precursor clusters to the substrate surface is the rate-determining step for scale crystal formation and growth, the calculated free energies of interaction of each substrate should display a negative relationship with gypsum scaling propensities, which follows the order as unmodified  $(-OH) < CH_3/C_6 < CH_3/C_{10} < CF_3/C_{10}$ . Such an order matches the results from gypsum scaling experiments (Figures 2B and 3B) and is similar to the findings discovered in the field of biomineralization that good binders are good nucleators. 55 Furthermore, the total free energies of interaction between CaSO<sub>4</sub> and substrate surface negatively correlate with the water contact angle (Figure 3C, red line) and positively correlate with the surface energy of the substrate surface (Figure 3C, blue line), both of which can be measured experimentally and used as indicators that predict surface scaling propensity.

The order of scaling propensities predicted by  $\Delta G_{\text{C-W-S}}$  could be explained by the varying interaction free energies of different substrates with water (Figure 3D, the detailed calculation is described in Text S2, Supporting Information). The surfaces with stronger hydrophilicity bind with water molecules more strongly, creating a more robust hydration layer that hinders the binding of  $\text{CaSO}_4$  precursor clusters with the substrate surface and thus reduces the surface scaling propensity. Conversely, the surfaces with higher hydrophobicity (e.g., the  $\text{CF}_3$ -terminated substrate) have a lower affinity with water molecules which in turn facilitate the adhesion of  $\text{CaSO}_4$  precursor clusters as well as the subsequent gypsum nucleation and crystal growth. Such a mechanism is analogous to that behind using hydrophilic surfaces to impart resistance against organic fouling.  $^{7,56-59}$ 

We noticed that the interaction between gypsum crystals and substrate surface has been used by Huang et al.<sup>23</sup> to explain surface propensity to gypsum scaling caused by homogeneous nucleation and bulk precipitation. In contrast, the analyses of this section focus on surface-mediated heterogeneous nucleation and are thus fundamentally different from those of Huang et al. Further, the existence of CaSO<sub>4</sub> precursor clusters during gypsum formation is essential to the validity of our findings discussed above. Several published studies have reported the presence of precursor clusters for mineral formation *via* the nonclassical pathway. 35,37,39 For example, Gebauer et al. 35 demonstrate the presence of prenucleation clusters for calcite formation by carefully performing potentiometric titration and analytical ultracentrifugation. Also, Stawski et al.<sup>37</sup> show that primary sub-3 nm CaSO<sub>4</sub> species exist during the first stage of gypsum formation using highly temporally resolved X-ray small- and wide-angle scattering experiment. The structure of those precursor clusters for gypsum has been derived using in situ high-energy X-ray diffraction experiments and molecular dynamics simulation.<sup>3</sup> Those fundamental studies in the field of mineralogy have provided solid evidence on the existence of precursor clusters for gypsum, consistent with the major viewpoint of this article.

**Implications and Prospects.** In this study, we combined theoretical and experimental investigations to understand the scaling propensity of surfaces with different wetting properties. According to CNT, more hydrophobic substrate surfaces hinder gypsum scaling underwater, but such theoretical predictions are inconsistent with experimental observations.

The predictions based on free energy of interaction between CaSO<sub>4</sub> and substrate surface match the experimental results, which implies that the adhesion of CaSO<sub>4</sub> species to the substrate may play an important role in heterogeneous CaSO<sub>4</sub> nucleation. Our work unveils new insights on the relationship between surface wetting property and scaling propensity, providing evidence that CNT, which has been used to understand mineral scaling in membrane desalination, <sup>19,21,23,60–62</sup> might not be applicable to describing surface scaling by gypsum. Instead, gypsum scaling is likely to occur *via* a nonclassical multistage process where the aggregation of precursor clusters and their interactions with substrate surface regulate gypsum nucleation and growth.

These findings improve our fundamental understanding of mineral scaling and may have important implications on the design of scaling-resistant membranes in desalination. In reverse osmosis (RO), hydrophilic surfaces are more favorable for designing membrane materials with high resistance to gypsum scaling, due to their lower affinity with CaSO<sub>4</sub> precursor clusters. This design criterion is consistent with the literature where hydrophilic polymers have been shown to improve membrane scaling resistance to gypsum scaling in RO desalination 24,25,63 and is compatible with the well-known principle of enhancing membrane fouling resistance via increasing surface hydrophilicity. 64,65 Therefore, it is possible to reconcile the design principles of fouling- and scalingresistant membranes to fabricate high-performance membranes for desalinating feedwaters having both high scaling and fouling potentials in RO.

However, it is worth mentioning that membrane technologies with distinct working principles might require different design principles of scaling-resistant membranes. In membrane distillation (MD), for example, superhydrophobic membranes are shown to be effective in resisting against gypsum scaling. 19-22 Since MD is suitable for the treatment of feedwaters with higher salinities than RO, MD membranes typically face higher concentrations of scalants, and thus, homogeneous nucleation plays a more important role in scale formation for MD than RO. Also, as microporous, hydrophobic membranes (contrasting to the dense, hydrophilic RO membranes) are used in MD, surface wettability of MD membranes regulates not only nucleation propensity but also water-membrane contact and boundary hydrodynamics. Our work suggests that the scaling resistance of superhydrophobic membranes in MD should not be due to the increase of freeenergy barrier to nucleation (which is suggested by several existing studies 19,21,66,67). Instead, membrane superhydrophobicity decreases the water-membrane contact area and creates a slip boundary condition. The former inhibits the deposition of scale particles or CaSO<sub>4</sub> precursor clusters; the latter enhances the crossflow velocity near the membrane surface and minimizes stagnant zones within partially wetted membrane pores, reducing both CaSO<sub>4</sub> precursor cluster attachment and concentration polarization. Therefore, future studies on the design of scaling-resistant membranes should consider the roles of nonclassical nucleation in governing scale formation (rather than only relying on CNT as the main theoretical guidance) and be tailored to the working principle of the membrane technology.

Despite the progress made in this study, mineral nucleation is a highly complicated process, and our study only provides evidence that CNT might not be able to describe the relationship between surface scaling propensity and wetting

property. More research efforts are needed to further elucidate the mechanisms of mineral scaling and the underlying nucleation pathway. For example, the model of CNT assumes a hemispherical nucleus that is valid for water vapor condensation. However, the validity of this assumption has not been proved for mineral nucleation in the aqueous solution, and the measurement of the nucleus-surface contact angle,  $\theta_{N/S}$ , has not been achieved by any current techniques. New approaches that more accurately reveal the geometrical nucleus-surface relation (e.g., via molecular simulation) may enable us to better understand the applicability of CNT to mineral nucleation in aqueous solutions. Also, mineral nucleation occurs at the nanoscale, whereas the surface energy components used in both CNT and the calculation of interaction free energy are typically obtained by contact angle measurements at the macroscale (the sizes of liquid droplets used in the measurement are millimeter in diameter). Despite the wide acceptance of using contact angle measurement to calculate surface energy components, 23,54,68-74 we acknowledge that the analyses in the current study are not able to capture surface chemistry heterogeneity (if any) at the nanoscale, which could alter local hydrophilicity. Therefore, future studies at finer resolutions or using patterned surfaces with defined hydrophilic and hydrophobic domains could better reveal the roles of surface wetting properties in regulating mineral scale formation.

Another question is whether the findings of the current study are applicable to other minerals such as calcite and silica. Indeed, different minerals have distinct formation mechanisms and behaviors. For example, the formation of calcite, which involves multiple types of amorphous CaCO3 (ACC) as the intermediate species,<sup>75</sup> is faster than gypsum, which prevents us from exclusively investigating surface-mediated, heterogeneous nucleation of calcite (Figure S6, Supporting Information). Also, silica is formed through a polymerization reaction (rather than crystallization reactions for gypsum and calcite), 76 and its amorphous nature is distinct from the crystalline nature of both gypsum and calcite.<sup>6</sup> Due to the complex differences among the formations of minerals, it is challenging to extrapolate the findings from one mineral (i.e., gypsum for the current study) to other minerals, and existing fundamental studies of mineral scaling typically focus on only one type of mineral. 23,50,51,55,77-79 Hence, more investigations are needed to probe the behaviors of surface-mediated mineral formation for other scaling types from the perspective of nucleation theory.

Furthermore, although more evidence has emerged to support the nonclassical nucleation pathway, <sup>17,33,34,38,80</sup> our knowledge on such a nucleation mechanism is still in its infancy. The existence of precursor clusters, which has been discussed above, has been typically reported for homogeneous nucleation in bulk solution. <sup>17,34,35,37,39</sup> This warrants future studies to investigate the presence and interactions of precursor clusters with substrate surfaces, as well as their effects on heterogeneous nucleation. Therefore, our study provides a first step toward a more complete, accurate understanding of heterogeneous mineral nucleation in aqueous solution, which is essential to the mitigation of mineral scaling in various industrial settings including membrane desalination.

#### ASSOCIATED CONTENT

#### Supporting Information

The Supporting Information is available free of charge at https://pubs.acs.org/doi/10.1021/acs.est.2c06560.

Surface tension components of water, ethylene glycol, diiodomethane, and gypsum; contact angles of water, ethylene glycol, and diiodomethane on different glass substrates with varied wetting properties; surface tension components of glass substrates calculated based on the contact angle measurements of water, ethylene glycol, and diiodomethane; relationship between the surfacearea-dependent term of CNT and the contact angle  $\theta_{\mathrm{N/S}}$ ; relationship of the contact angle  $\theta_{\mathrm{N/S}}$  with the total surface energy and the water contact angle of the glass substrate; XPS characterization of the unmodified substrate and substrates modified with different functional silanes; measurement of gypsum solution conductivity without glass slides for 2 days; measurement of calcite solution conductivity without glass slide samples for 24 h; text for the mathematical derivation of eq 4 of the main text; and text for the calculation of interaction free energy between different substrates and water (PDF)

#### AUTHOR INFORMATION

#### **Corresponding Author**

Tiezheng Tong — Department of Civil and Environmental Engineering, Colorado State University, Fort Collins, Colorado 80523, United States; orcid.org/0000-0002-9289-3330; Phone: +1(970)491-1913; Email: tiezheng.tong@colostate.edu

#### **Authors**

Yiming Yin — Department of Civil and Environmental Engineering, Colorado State University, Fort Collins, Colorado 80523, United States

Tianshu Li — Department of Civil and Environmental Engineering, George Washington University, Washington, District of Columbia 20052, United States; orcid.org/0000-0002-0529-543X

Kuichang Zuo — The Key Laboratory of Water and Sediment Science, Ministry of Education; College of Environment Science and Engineering, Peking University, Beijing 100871, China; ⊚ orcid.org/0000-0002-3922-8702

Xitong Liu — Department of Civil and Environmental Engineering, George Washington University, Washington, District of Columbia 20052, United States; ⊚ orcid.org/0000-0002-5197-3422

Shihong Lin − Department of Civil and Environmental Engineering, Vanderbilt University, Nashville, Tennessee 37212, United States; ⑤ orcid.org/0000-0001-9832-9127

Yiqun Yao — Department of Civil and Environmental Engineering, Colorado State University, Fort Collins, Colorado 80523, United States

Complete contact information is available at: https://pubs.acs.org/10.1021/acs.est.2c06560

#### Notes

The authors declare no competing financial interest.

#### ACKNOWLEDGMENTS

The authors acknowledge the support from the start-up funds that T.T. received from the Department of Civil and Environmental Engineering, College of Engineering, at Colorado State University. This material is also based upon work partially supported by the National Science Foundation *via* Grant No. 2145627 and the National Alliance for Water Innovation (NAWI), funded by the U.S. Department of Energy, Energy Efficiency and Renewable Energy Office, Advanced Manufacturing Office under Funding Opportunity Announcement DE-FOA-0001905. The views expressed herein do not necessarily represent the views of the National Science Foundation, the U.S. Department of Energy, or the United States Government.

#### REFERENCES

- (1) Reznikov, N.; Steele, J.; Fratzl, P.; Stvens, M. A materials science vision of extracellular matrix mineralization. *Nat. Rev. Mater.* **2016**, *1*, No. 16041.
- (2) Liu, X. Y. Heterogeneous nucleation or homogeneous nucleation? J. Chem. Phys. 2000, 112, 9949–9955.
- (3) Putnis, A. Why mineral interfaces matter. Science 2014, 343, 1441–1442.
- (4) De Yoreo, J. J.; Sommerdijk, N. A.; Dove, P. M.Nucleation Pathways in Electrolyte Solutions. In *New Perspectives on Mineral Nucleation and Growth*; Springer, 2017; pp 1–24.
- (5) Fletcher, R. C.; Merino, E. Mineral growth in rocks: Kinetic-rheological models of replacement, vein formation, and syntectonic crystallization. *Geochim. Cosmochim. Acta* **2001**, *65*, 3733–3748.
- (6) Tong, T.; Wallace, A. F.; Zhao, S.; Wang, Z. Mineral scaling in membrane desalination: Mechanisms, mitigation strategies, and feasibility of scaling-resistant membranes. *J. Membr. Sci.* **2019**, *579*, 52–69
- (7) Horseman, T.; Yin, Y.; Christie, K. S.; Wang, Z.; Tong, T.; Lin, S. Wetting, scaling, and fouling in membrane distillation: State-of-theart insights on fundamental mechanisms and mitigation strategies. ACS ES&T Eng. 2021, 1, 117–140.
- (8) Dhyani, A.; Wang, J.; Halvey, A. K.; Macdonald, B.; Mehta, G.; Tuteja, A. Design and applications of surfaces that control the accretion of matter. *Science* **2021**, *373*, No. eaba5010.
- (9) McBride, S. A.; Girard, H.-L.; Varanasi, K. K. Crystal critters: Self-ejection of crystals from heated, superhydrophobic surfaces. *Sci. Adv.* **2021**, *7*, No. eabe6960.
- (10) McBride, S. A.; Dash, S.; Varanasi, K. K. Evaporative crystallization in drops on superhydrophobic and liquid-impregnated surfaces. *Langmuir* **2018**, *34*, 12350–12358.
- (11) Antony, A.; Low, J. H.; Gray, S.; Childress, A. E.; Le-Clech, P.; Leslie, G. Scale formation and control in high pressure membrane water treatment systems: A review. *J. Membr. Sci.* **2011**, 383, 1–16.
- (12) Rolf, J.; Cao, T.; Huang, X.; Boo, C.; Li, Q.; Elimelech, M. Inorganic Scaling in Membrane Desalination: Models, Mechanisms, and Characterization Methods. *Environ. Sci. Technol.* **2022**, *56*, 7484–7511
- (13) Zanotto, E. D.; James, P. F. Experimental tests of the classical nucleation theory for glasses. *J. Non-Cryst. Solids* **1985**, *74*, 373–394. (14) Niu, H.; Piaggi, P. M.; Invernizzi, M.; Parrinello, M. Molecular dynamics simulations of liquid silica crystallization. *Proc. Natl. Acad. Sci.* **2018**, *115*, 5348–5352.
- (15) Wette, P.; Schöpe, H. J. Nucleation kinetics in deionized charged colloidal model systems: A quantitative study by means of classical nucleation theory. *Phys. Rev. E* **2007**, *75*, No. 051405.
- (16) Lundrigan, S. E. M.; Saika-Voivod, I. Test of classical nucleation theory and mean first-passage time formalism on crystallization in the Lennard-Jones liquid. *J. Chem. Phys.* **2009**, *131*, No. 104503.
- (17) Karthika, S.; Radhakrishnan, T.; Kalaichelvi, P. A review of classical and nonclassical nucleation theories. *Cryst. Growth Des.* **2016**, *16*, *6663–6681*.

- (18) Kalikmanov, V. I.Classical Nucleation Theory. In *Nucleation Theory*; Springer, 2013; pp 17-41.
- (19) Xiao, Z.; Li, Z.; Guo, H.; Liu, Y.; Wang, Y.; Yin, H.; Li, X.; Song, J.; Nghiem, L. D.; He, T. Scaling mitigation in membrane distillation: From superhydrophobic to slippery. *Desalination* **2019**, 466, 36–43.
- (20) Wang, S.; Xiao, K.; Huang, X. Characterizing the roles of organic and inorganic foulants in RO membrane fouling development: The case of coal chemical wastewater treatment. *Sep. Purif. Technol.* **2019**, *210*, 1008–1016.
- (21) Karanikola, V.; Boo, C.; Rolf, J.; Elimelech, M. Engineered slippery surface to mitigate gypsum scaling in membrane distillation for treatment of hypersaline industrial wastewaters. *Environ. Sci. Technol.* **2018**, *52*, 14362–14370.
- (22) Su, C.; Horseman, T.; Cao, H.; Christie, K.; Li, Y.; Lin, S. Robust superhydrophobic membrane for membrane distillation with excellent scaling resistance. *Environ. Sci. Technol.* **2019**, *53*, 11801–11809.
- (23) Huang, X.; Li, C.; Zuo, K.; Li, Q. Predominant effect of material surface hydrophobicity on gypsum scale formation. *Environ. Sci. Technol.* **2020**, *54*, 15395–15404.
- (24) Cao, B.; Stack, A. G.; Steefel, C. I.; DePaolo, D. J.; Lammers, L. N.; Hu, Y. D. Investigating calcite growth rates using a quartz crystal microbalance with dissipation (QCM-D). *Geochim. Cosmochim. Acta* 2018, 222, 269–283.
- (25) Jaramillo, H.; Boo, C.; Hashmi, S. M.; Elimelech, M. Zwitterionic coating on thin-film composite membranes to delay gypsum scaling in reverse osmosis. *J. Membr. Sci.* **2021**, *618*, No. 118568.
- (26) Zhang, T.; Wang, Y.; Zhang, F.; Chen, X.; Hu, G.; Meng, J.; Wang, S. Bio-inspired superhydrophilic coatings with high anti-adhesion against mineral scales. *NPG Asia Mater.* **2018**, *10*, No. e471.
- (27) Meng, J.; Wang, S. Advanced antiscaling interfacial materials toward highly efficient heat energy transfer. *Adv. Funct. Mater.* **2020**, 30, No. 1904796.
- (28) Volmer, M.; Weber, A. Keimbildung in übersättigten Gebilden. Z. Phys. Chem. 1926, 119, 277-301.
- (29) Becker, R.; Döring, W. Kinetische behandlung der keimbildung in übersättigten dämpfen. Ann. Phys. 1935, 416, 719–752.
- (30) Frenkel, J. A general theory of heterophase fluctuations and pretransition phenomena. J. Chem. Phys. 1939, 7, 538-547.
- (31) Bi, Y.; Cabriolu, R.; Li, T. Heterogeneous ice nucleation controlled by the coupling of surface crystallinity and surface hydrophilicity. *J. Phys. Chem. C* **2016**, *120*, 1507–1514.
- (32) Cabriolu, R.; Li, T. Ice nucleation on carbon surface supports the classical theory for heterogeneous nucleation. *Phys. Rev. E* **2015**, *91*, No. 052402.
- (33) Erdemir, D.; Lee, A. Y.; Myerson, A. S. Nucleation of crystals from solution: Classical and two-step models. *Acc. Chem. Res.* **2009**, 42, 621–629.
- (34) Meldrum, F. C.; Sear, R. P. Now you see them. *Science* **2008**, 322, 1802–1803.
- (35) Gebauer, D.; Völkel, A.; Cölfen, H. Stable prenucleation calcium carbonate clusters. *Science* **2008**, 322, 1819–1822.
- (36) De Yoreo, J. J.; Waychunas, G. A.; Jun, Y.-S.; Fernandez-Martinez, A. In situ investigations of carbonate nucleation on mineral and organic surfaces. *Rev. Mineral. Geochem.* **2013**, *77*, 229–257.
- (37) Stawski, T. M.; van Driessche, A. E. S.; Ossorio, M.; Diego Rodriguez-Blanco, J.; Besselink, R.; Benning, L. G. Formation of calcium sulfate through the aggregation of sub-3 nanometre primary species. *Nat. Commun.* **2016**, *7*, No. 11177.
- (38) Gebauer, D.; Cölfen, H. Prenucleation clusters and non-classical nucleation. *Nano Today* **2011**, *6*, 564–584.
- (39) Stawski, T. M.; Van Driessche, A. E.; Besselink, R.; Byrne, E. H.; Raiteri, P.; Gale, J. D.; Benning, L. G. The structure of CaSO<sub>4</sub> nanorods: The precursor of gypsum. *J. Phys. Chem. C* **2019**, *123*, 23151–23158.

- (40) Christie, K. S. S.; Yin, Y.; Lin, S.; Tong, T. Distinct behaviors between gypsum and silica scaling in membrane distillation. *Environ. Sci. Technol.* **2020**, *54*, 568–576.
- (41) Krumpfer, J. W.; McCarthy, T. J. Rediscovering silicones: "unreactive" silicones react with inorganic surfaces. *Langmuir* **2011**, *27*, 11514–11519.
- (42) Van Oss, C. Acid-base interfacial interactions in aqueous media. *Colloids Surf., A* 1993, 78, 1–49.
- (43) Greczynski, G.; Hultman, L. C 1s peak of adventitious carbon aligns to the vacuum level: Dire consequences for material's bonding assignment by photoelectron spectroscopy. *ChemPhysChem* **2017**, *18*, 1507–1512.
- (44) Parkhurst, D. L.User's Guide to PHREEQC: A Computer Program for Speciation, Reaction-Path, Advective-Transport, and Inverse Geochemical Calculations. In *US Department of the Interior*; US Geological Survey, 1995; Vol. 95.
- (45) Ferreira, T.; Rasband, W.ImageJ/Fiji. ImageJ User Guide, version 1.44, 2012 Vol. 1, pp 155–161.
- (46) Clouet, E.Modeling of Nucleation Processes. 2010. arXiv:1001.4131. arXiv.org e-Print archive. https://doi.org/10.48550/arXiv.1001.4131.
- (47) Prisciandaro, M.; Olivieri, E.; Lancia, A.; Musmarra, D. PBTC as an antiscalant for gypsum precipitation: Interfacial tension and activation energy estimation. *Ind. Eng. Chem. Res.* **2012**, *51*, 12844–12851.
- (48) Hina, A.; Nancollas, G.; Grynpas, M. Surface induced constant composition crystal growth kinetics studies. The brushite—gypsum system. *J. Cryst. Growth* **2001**, 223, 213–224.
- (49) Christie, K. S.; Horseman, T.; Wang, R.; Su, C.; Tong, T.; Lin, S. Gypsum scaling in membrane distillation: Impacts of temperature and vapor flux. *Desalination* **2022**, *525*, No. 115499.
- (50) Wang, Y.-W.; Kim, Y.-Y.; Christenson, H. K.; Meldrum, F. C. A new precipitation pathway for calcium sulfate dihydrate (gypsum) via amorphous and hemihydrate intermediates. *Chem. Commun.* **2012**, 48, 504–506.
- (51) Van Driessche, A. E. S.; Benning, L. G.; Rodriguez-Blanco, J.; Ossorio, M.; Bots, P.; García-Ruiz, J. The role and implications of bassanite as a stable precursor phase to gypsum precipitation. *Science* **2012**, 336, 69–72.
- (52) Van Santen, R. A. The Ostwald step rule. J. Phys. Chem. A 1984, 88, 5768-5769.
- (53) Van Oss, C. J.Interfacial Forces in Aqueous Media; CRC press,
- (54) Teng, F.; Zeng, H.; Liu, Q. Understanding the deposition and surface interactions of gypsum. *J. Phys. Chem. C* **2011**, *115*, 17485–17494.
- (55) Hamm, L. M.; Giuffre, A. J.; Han, N.; Tao, J. H.; Wang, D. B.; De Yoreo, J. J.; Dove, P. M. Reconciling disparate views of template-directed nucleation through measurement of calcite nucleation kinetics and binding energies. *Proc. Natl. Acad. Sci. U.S.A.* **2014**, *111*, 1304–1309.
- (56) Zhang, R.; Liu, Y.; He, M.; Su, Y.; Zhao, X.; Elimelech, M.; Jiang, Z. Antifouling membranes for sustainable water purification: strategies and mechanisms. *Chem. Soc. Rev.* **2016**, *45*, 5888–5924.
- (57) Liu, C.; Lee, J.; Ma, J.; Elimelech, M. Antifouling thin-film composite membranes by controlled architecture of zwitterionic polymer brush layer. *Environ. Sci. Technol.* **2017**, *51*, 2161–2169.
- (58) Lee, J.; Chae, H.-R.; Won, Y. J.; Lee, K.; Lee, C.-H.; Lee, H. H.; Kim, I.-C.; Lee, J.-m. Graphene oxide nanoplatelets composite membrane with hydrophilic and antifouling properties for wastewater treatment. *J. Membr. Sci.* **2013**, *448*, 223–230.
- (59) Wang, Z.; Elimelech, M.; Lin, S. Environmental applications of interfacial materials with special wettability. *Environ. Sci. Technol.* **2016**, *50*, 2132–2150.
- (60) Liu, L.; Xiao, Z.; Liu, Y.; Li, X.; Yin, H.; Volkov, A.; He, T. Understanding the fouling/scaling resistance of superhydrophobic/omniphobic membranes in membrane distillation. *Desalination* **2021**, 499, No. 114864.

- (61) Horseman, T.; Su, C.; Christie, K. S.; Lin, S. Highly effective scaling mitigation in membrane distillation using a superhydrophobic membrane with gas purging. *Environ. Sci. Technol. Lett.* **2019**, *6*, 423–429.
- (62) Chen, Y.; Lu, K. J.; Chung, T.-S. An omniphobic slippery membrane with simultaneous anti-wetting and anti-scaling properties for robust membrane distillation. *J. Membr. Sci.* **2020**, 595, No. 117572.
- (63) Kim, M.-m.; Lin, N. H.; Lewis, G. T.; Cohen, Y. Surface nanostructuring of reverse osmosis membranes via atmospheric pressure plasma-induced graft polymerization for reduction of mineral scaling propensity. *J. Membr. Sci.* **2010**, 354, 142–149.
- (64) She, Q.; Wang, R.; Fane, A. G.; Tang, C. Y. Membrane fouling in osmotically driven membrane processes: A review. *J. Membr. Sci.* **2016**, 499, 201–233.
- (65) Jiang, S.; Li, Y.; Ladewig, B. P. A review of reverse osmosis membrane fouling and control strategies. *Sci. Total Environ.* **2017**, 595, 567–583.
- (66) Liao, X.; Dai, P.; Wang, Y.; Zhang, X.; Liao, Y.; You, X.; Razaqpur, A. G. Engineering anti-scaling superhydrophobic membranes for photothermal membrane distillation. *J. Membr. Sci.* **2022**, 650, No. 120423.
- (67) Zheng, G.; Yao, L.; You, X.; Liao, Y.; Wang, R.; Huang, J. J. Effects of different secondary nano-scaled roughness on the properties of omniphobic membranes for brine treatment using membrane distillation. *J. Membr. Sci.* **2021**, *620*, No. 118918.
- (68) Hefer, A. W.; Bhasin, A.; Little, D. N. Bitumen surface energy characterization using a contact angle approach. *J. Mater. Civil Eng.* **2006**, *18*, 759–767.
- (69) Clint, J. H. Adhesion and components of solid surface energies. *Curr. Opin. Colloid Interface Sci.* **2001**, *6*, 28–33.
- (70) Binks, B. P.; Clint, J. H. Solid wettability from surface energy components: relevance to Pickering emulsions. *Langmuir* **2002**, *18*, 1270–1273.
- (71) Kozbial, A.; Li, Z.; Conaway, C.; McGinley, R.; Dhingra, S.; Vahdat, V.; Zhou, F.; D'Urso, B.; Liu, H.; Li, L. Study on the surface energy of graphene by contact angle measurements. *Langmuir* **2014**, 30, 8598–8606.
- (72) Kühnl, W.; Piry, A.; Kaufmann, V.; Grein, T.; Ripperger, S.; Kulozik, U. Impact of colloidal interactions on the flux in cross-flow microfiltration of milk at different pH values: A surface energy approach. J. Membr. Sci. 2010, 352, 107–115.
- (73) Brack, H. P.; Wyler, M.; Peter, G.; Scherer, G. G. A contact angle investigation of the surface properties of selected proton-conducting radiation-grafted membranes. *J. Membr. Sci.* **2003**, 214, 1–19.
- (74) Brant, J. A.; Childress, A. E. Assessing short-range membrane—colloid interactions using surface energetics. *J. Membr. Sci.* **2002**, 203, 257–273.
- (75) Cartwright, J. H. E.; Checa, A. G.; Gale, J. D.; Gebauer, D.; Sainz-Díaz, C. I. Calcium carbonate polyamorphism and its role in biomineralization: How many amorphous calcium carbonates are there? *Angew. Chem., Int. Ed.* **2012**, *51*, 11960–11970.
- (76) Milne, N. A.; O'Reilly, T.; Sanciolo, P.; Ostarcevic, E.; Beighton, M.; Taylor, K.; Mullett, M.; Tarquin, A. J.; Gray, S. R. Chemistry of silica scale mitigation for RO desalination with particular reference to remote operations. *Water Res.* **2014**, *65*, 107–133.
- (77) Cao, T.; Rolf, J.; Wang, Z.; Violet, C.; Elimelech, M. Distinct impacts of natural organic matter and colloidal particles on gypsum crystallization. *Water Res.* **2022**, *218*, No. 118500.
- (78) Shaffer, D. L.; Tousley, M. E.; Elimelech, M. Influence of polyamide membrane surface chemistry on gypsum scaling behavior. *J. Membr. Sci.* **2017**, *525*, 249–256.
- (79) Giuffre, A. J.; Hamm, L. M.; Han, N.; De Yoreo, J. J.; Dove, P. M. Polysaccharide chemistry regulates kinetics of calcite nucleation through competition of interfacial energies. *Proc. Natl. Acad. Sci.* **2013**, 110, 9261–9266.
- (80) De Yoreo, J. More than one pathway. Nat. Mater. 2013, 12, 284-285.

### **□** Recommended by ACS

Wettability of NaNO<sub>3</sub> and KNO<sub>3</sub> on MgO and Carbon Surfaces—Understanding the Substrate and the Length Scale Effects

A. Anagnostopoulos, Y. Ding, et al.

MARCH 19, 2020

THE JOURNAL OF PHYSICAL CHEMISTRY C

DEAD E

## **Bassanite Grows Along Distinct Coexisting Pathways and Provides a Low Energy Interface for Gypsum Nucleation**

Caiyun Jia, James J. De Yoreo, et al.

OCTOBER 11, 2022

CRYSTAL GROWTH & DESIGN

READ 🗹

## Process-Specific Effects of Sulfate on CaCO<sub>3</sub> Formation in Environmentally Relevant Systems

Yaguang Zhu, Young-Shin Jun, et al.

MAY 26, 2022

ENVIRONMENTAL SCIENCE & TECHNOLOGY

READ 🗹

#### Phase State and Relative Humidity Regulate the Heterogeneous Oxidation Kinetics and Pathways of Organic-Inorganic Mixed Aerosols

Chuanyang Shen, Haofei Zhang, et al.

OCTOBER 28, 2022

ENVIRONMENTAL SCIENCE & TECHNOLOGY

READ 🗹

Get More Suggestions >